THE JOURNAL OF BIOLOGICAL CHEMISTRY
Vol. 265, No. 2, Issue of January 15, pp. 652-659, 1990
Printed in U.S.A.

Kinetic Studies on Spin Trapping of Superoxide and Hydroxyl Radicals Generated in NADPH-Cytochrome P-450 Reductase-Paraquat Systems

EFFECT OF IRON CHELATES*

(Received for publication, March 8, 1989)

Isao Yamazaki‡, Lawrence H. Piette, and Thomas A. Grover

From the Department of Chemistry and Biochemistry, Utah State University, Logan, Utah 84322-0300

Electron spin resonance (ESR) studies on spin trapping of superoxide and hydroxyl radicals by 5,5-dimethyl-1-pyrroline-1-oxide (DMPO) were performed in NADPH-cytochrome P-450 reductase-paraquat systems at pH 7.4. Spin adduct concentrations were determined by comparing ESR spectra of the adducts with the ESR spectrum of a stable radical solution. Kinetic analysis in the presence of 100 μM desferrioxamine B (deferoxamine) showed that: 1) the oxidation of 1 mol of NADPH produces 2 mol of superoxide ions, all of which can be trapped by DMPO when extrapolated to infinite concentration; 2) the rate constant for the reaction of superoxide with DMPO was 1.2 M^{-1} s^{-1}; 3) the superoxide spin adduct of DMPO (DMPO-OOH) decays with a half-life of 66 s and the maximum level of DMPO-OOH formed can be calculated by a simple steady state equation; and 4) 2.8% or less of the DMPO-OOH decay occurs through a reaction producing hydroxyl radicals.

In the presence of 100 μM EDTA, 5 μM Fe(III) ions nearly completely inhibited the formation of the hydroxyl radical adduct of DMPO (DMPO-OH) as well as the formation of DMPO-OOH and, when 100 μM hydrogen peroxide was present, produced DMPO-OH exclusively. Fe(III)-EDTA is reduced by superoxide and the competition of superoxide and hydrogen peroxide in the reaction with Fe(II)-EDTA seems to be reflected in the amounts of DMPO-OOH and DMPO-OH detected. These effects of EDTA can be explained from known kinetic data including a rate constant of 6 × 10^4 M^{-1} s^{-1} for reduction of DMPO-OOH by Fe(II)-EDTA. The effect of diethylenetriamine pentaacetic acid (DETAPAC) on the formation of DMPO-OOH and DMPO-OH was between deferoxamine and EDTA, and about the same as that of endogenous chelator (phosphate).

Superoxide is produced in biological systems via various enzymatic and nonenzymatic reactions. Although superoxide itself produces some biological effects (1), it is now well accepted that the most deleterious effects of oxygen radicals are caused by hydroxyl radicals produced from iron-catalyzed Haber-Weiss reactions. This conclusion has been derived from a myriad of reports (2), which have accumulated since the superoxide dismutase, once isolated from erythrocytes on the basis of its activity, was found to be identical to erythrocuprein (3). Superoxide formed in biochemical systems has been assayed by following its reactions with horseradish peroxidase (4), lactoperoxidase (5), myeloperoxidase (6), diacetyldeutero-substituted horseradish peroxidase (7), acetylated cytochrome *c* (8), succinoylated cytochrome *c* (9), and some organic molecules (10, 11). Hydroxyl radicals formed in biochemical systems can be assayed chemically with *p*-nitrosodimethylaniline (12), benzoate (13), salicylate (14), 2-keto-4-thiomethylbutyrate (15), and circular DNA (16). However, electron spin resonance (ESR) has provided powerful and unambiguous techniques for detecting these oxygen radicals. Superoxide is detected directly by ESR in frozen solutions (17, 18), but during the last decade spin-trapping methods have been extensively used to detect oxygen radicals with 5,5-dimethyl-1-pyrroline-1-oxide (DMPO)[1] (19–22) and α-phenyl-*N*-*tert*-butyl nitrone (21–23).

Most of these spin-trapping studies, however, are qualitative. For the generation of oxygen radicals in biochemical systems, some investigators (20, 24–30) have reported kinetic data based on the relative intensity of ESR signals and only a few papers have reported a molar concentration for the amount of superoxide adduct of DMPO (DMPO-OOH) (31–32) or hydroxyl radical adduct of DMPO (DMPO-OH) (32–33). In spite of the fact that hydroxyl radical generation is closely related to superoxide formation, there is no kinetic and quantitative data that deal with the relationship between superoxide and hydroxyl radicals, except that of Finkelstein *et al.* (34) who reported the production of hydroxyl radical by decomposition of DMPO-OOH. Since the amount of such oxygen-radical adducts detected by ESR is only a part of the overall biochemical metabolites produced, it is necessary to elucidate kinetic meanings of the spin detection in the overall metabolism.

To clarify the quantitative relationships between enzymatic reactions and spin-trapping data of oxygen radicals, we have used the NADPH-cytochrome P-450 reductase-paraquat system as a standard system, since the primary reduction product of oxygen is thought to be only superoxide. For instance, xanthine oxidase, a widely used superoxide-generating enzyme produces both superoxide ions and hydrogen peroxide as primary products (5, 35) and the kinetic analysis is considerably more complex.

Several papers have reported that the Haber-Weiss reaction is too slow to explain the formation of hydroxyl radicals in

* The costs of publication of this article were defrayed in part by the payment of page charges. This article must therefore be hereby marked "*advertisement*" in accordance with 18 U.S.C. Section 1734 solely to indicate this fact.

‡ To whom all correspondence should be addressed.

[1] The abbreviations and trivial names used are: DMPO, 5,5-dimethyl-1-pyrroline-1-oxide; DMPO-OOH, superoxide adduct of DMPO; DMPH-OH, hydroxyl radical adduct of DMPO; deferoxamine, desferrioxamine B; DETAPAC, diethylenetriamine pentaacetic acid.

biological systems (36) and it is now well accepted that iron plays an essential role in the formation of hydroxyl radicals from superoxide-generating systems. Since the role of iron is greatly modified by its chelators, we have attempted to examine the effects of three typical iron chelators, desferrioxamine B (deferoxamine), diethylenetriamine pentaacetic acid (DETAPAC), and EDTA.

EXPERIMENTAL PROCEDURES AND RESULTS[2]

DISCUSSION

Paraquat-mediated superoxide generation has been reported in NADPH-cytochrome P-450 reductase systems (58), glutathione reductase systems (41), animal systems (59, 60), plant systems (28, 61), and microorganisms (44, 62, 63). It is believed that reducing equivalents accepted by paraquat are all used to reduce oxygen to superoxide ions, but without any quantitative evidence. The kinetic data in Fig. 5 show that within experimental errors the following stoichiometry is established in the NADPH-cytochrome P-450 reductase-paraquat system,

$$NADPH + 2\ O_2 \rightarrow NADP^+ + H^+ + 2\ O_2^-,$$

and also that all the resultant superoxide ions can be trapped by DMPO when extrapolated to infinite DMPO concentration. The slopes in Fig. 5 give a value of 2.2×10^5 M·s for k_d/k_2^2, which is much higher than the value of 3×10^3 M·s obtained using data of $k_d = 3 \times 10^5$ M^{-1} s^{-1} (64) and $k_2 = 10$ M^{-1} s^{-1} (31) at pH 7.4. If one assumes that the k_d value is correct, the k_2 value will be about 1.2 M^{-1} s^{-1}, which is significantly less than that reported by Finkelstein *et al.* (31). This difference is probably, in part, ascribable to the difference in the experimental conditions (ionic strength, iron chelator, etc.) The DMPO concentration that traps one-half of the superoxide ions accumulated increases with the increase in the rate of superoxide formation as can be seen in Fig. 5 and Table II.

For the DMPO-OOH decay we conclude as follows: 1) DMPO-OOH decays with a half-life of 66 s ($k_1 = 0.011$ s^{-1}) at pH 7.4 according to first order kinetics. The rate is nearly the same as that obtained in illuminated pea chloroplasts at pH 7 (28). 2) the DMPO-OOH decay is accompanied by the production of a small amount of DMPO-OH. The conversion ratio is measured to be 2.8%, that is, 0.8 μM DMPO-OH is formed during the decay of 29 μM DMPO-OOH, which is equal to the approximate integrated value, $\int k_1$[DMPO-OOH] dt, obtained from the kinetic trace for formation and decay of DMPO-OOH as shown in Fig. 4*A*. Here, a value of 0.011 s^{-1} is used for k_1. The total amount of DMPO-OOH formed during the reaction will be greater than 29 μM since k_1 appears to be greater than 0.011 s^{-1} under these experimental conditions (Table I). DMPO-OH is assumed to be stable under these conditions. Since Fig. 6*C* shows that DMPO-OH is formed through the reaction of DMPO with hydroxyl radicals, we conclude that 2.8% or less of DMPO-OOH decay occurs through a reaction producing hydroxyl radicals. Finkelstein *et al.* (34) have reported that the ratio is about 3%. The formation of DMPO-OH from DMPO-OOH has been discussed also in neutrophil systems (65). 3) DMPO-OOH reaches a steady level a few minutes after initiation of the reactions in the presence of 5–10 μM paraquat (Fig. 2). Equation 1 is valid under these experimental conditions.

The above conclusions are obtained from reactions in the presence of 100 μM deferoxamine. According to recent reports (66, 67), deferoxamine reacts with both superoxide ions and hydroxyl radicals, with rate constants of 9×10^2 and 10^{10} M^{-1} s^{-1}, respectively. These reactions may be negligible in our reaction systems since the concentration of DMPO is 1000 times higher than that of deferoxamine and we could not observe any nitroxide-free radical which is a product of the reaction of deferoxamine with superoxide (67). When deferoxamine is present, the mechanism of oxygen metabolism in the NADPH-cytochrome P-450 reductase-paraquat system is relatively simple as shown in Fig. 14*A*. The formation of hydroxyl radicals through reactions of hydrogen peroxide with superoxide and paraquat radicals is not detectable under our experimental conditions.

The reaction becomes complicated in the presence of Fe(III)-EDTA, which has been used most frequently as a Fenton reagent. The complication arises not only from the Fenton reaction, but also from reactions of Fe(II)-EDTA with superoxide, hydrogen peroxide, and DMPO-OOH. Fig. 14*B* shows a mechanism schematized using data so far reported

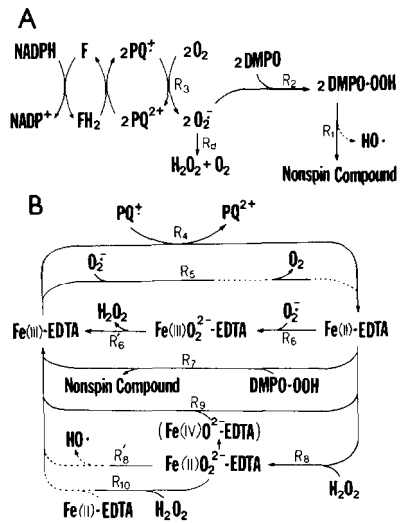

FIG. 14. **Proposed scheme for formation of DMPO-OOH and DMPO-OH in the NADPH-cytochrome P-450 reductase-paraquat system.** The rate constants referenced are at neutral pH (mostly pH 7.4). *A*, reactions in the presence of deferoxamine and *B*, effect of Fe(III)-EDTA. $k_d = 3 \times 10^5$ M^{-1} s^{-1} (64). R_1, decomposition of DMPO-OOH which yields mostly nonspin, not identified compound(s). The *dotted line* denotes a side reaction yielding hydroxyl radicals which can be spin trapped with DMPO. The molar ratio of DMPO-OH formed per DMPO-OOH is about 0.03 (34; this paper). $k_1 = 0.011$ s^{-1} (28; this paper). R_2, spin trapping of superoxide ions by DMPO. $k_2 = 10$ M^{-1} s^{-1} (31) and 1.2 M^{-1} s^{-1} (this paper). R_3, reduction of O_2 by paraquat radicals. $k_3 = 7.7 \times 10^8$ M s^{-1} (68). R_4, reduction of Fe(III)-EDTA by paraquat radicals. The reaction is assumed to be fast (71). R_5, reduction of Fe(III)-EDTA by superoxide. The reaction is pH dependent and $k_5 = 1\text{–}2 \times 10^6$ M^{-1} s^{-1} (50, 69). The *dotted line* implies that R_5 takes place through an unknown encounter complex (50). R_6, reaction of Fe(II)-EDTA with a superoxide ion to form a peroxo-complex. $k_6 = 10^6$ 10^7 M^{-1} s^{-1} (50, 69). R_6', reversible complexing of Fe(III)-EDTA and H_2O_2 (50). k_6' depends greatly on pH and the kind of buffers used (50). R_7, reduction of DMPO-OOH by Fe(II)-EDTA to a nonspin compound. $k_7 = 6 \times 10^4$ M^{-1} s^{-1} (this paper). R_8, reaction of Fe(II)-EDTA with H_2O_2 forming an oxidizing intermediate, which might be converted to a ferryl form, Fe(IV)O^{2+}-EDTA, or produce a hydroxyl radical (R_8'). $k_8 = 2 \times 10^4$ M^{-1} s^{-1} (50), 1.74×10^4 M^{-1} s^{-1} (52), and 7×10^3 M^{-1} s^{-1} (53). R_9, reduction of Fe(IV)O^{2+}-EDTA by Fe(II)-EDTA (52, 53). R_{10}, formation of a second oxidizing transient in the reaction of Fe(II)-EDTA with H_2O_2. $k_{10} = 3.2 \times 10^3$ M^{-1} s^{-1} (52). The *dotted line* implies that the detailed mechanism is not yet clear.

[2] Portions of this paper (including "Experimental Procedures," "Results," Figs. 1–13, and Tables I–III) are presented in miniprint at the end of this paper. Miniprint is easily read with the aid of a standard magnifying glass. Full size photocopies are included in the microfilm edition of the Journal that is available from Waverly Press.

(47–55, 68–71). The following features of Fe(III)-EDTA reactions may be explained by the calculated approximate rates of reactions.

1) Although Reaction 4 is reported to be rapid (71), paraquat radicals reduce exclusively oxygen (Reaction 3) rather than Fe(III)-EDTA (Reaction 4), when the Fe(III)-EDTA concentration is less than 5 μM.

2) When the superoxide generation is slow, 5 μM Fe(III)-EDTA completely inhibits the DMPO-OOH accumulation (Fig. 8*C*). As seen in Fig. 14*B*, this inhibition may occur through two mechanisms, one is reductive decomposition of DMPO-OOH by Fe(II)-EDTA (Reaction 7) and the other is a weak superoxide dismutase activity of iron-EDTA (Reactions 5, 6, and 6′). The superoxide dismutase activity of Fe(III)-EDTA is still controversial mostly because of the apparent slow dissociation of an iron-EDTA-peroxide complex (Reaction 6′). At pH 7.4, the value for k_6' is estimated to be at least 1 s^{-1} or possibly larger (48, 50). The rate constant of 1 s^{-1} would be very slow for iron-EDTA to catalyze the dismutation of superoxide ions at any significant rate under the usual assay conditions for O_2^- as described by Diguiseppi and Fridovich (54). Under the experimental conditions in Fig. 8*C* where the rate of superoxide formation is about 0.2 μM s^{-1} (Table I) and the rate of reaction of DMPO with superoxide ions is very slow, calculations using the known rate constants shown in the legend of Fig. 14 and using a value of 1 s^{-1} for k_6' clearly show that the maximal DMPO-OOH accumulation is decreased from 6.2 (Table I) to 0.23 μM through Reactions 5, 6, and 6′ in the presence of 5 μM iron-EDTA. Under the same conditions the DMPO-OOH concentration would decrease to about one-sixth the original concentration following Reaction 7 alone. Since these two mechanisms operate additively, the DMPO-OOH accumulation following both decay mechanisms would be expected to decrease to a level below the ESR sensitivity (Table III). As the superoxide generation becomes faster, superoxide ions disappear mostly through dismutation and more Fe(III)-EDTA is needed for complete suppression of DMPO-OOH formation (Fig. 11*A*).

3) Reaction of the Fe(II)-EDTA is switched from Reaction 6 to Reaction 8 by the presence of 100 μM hydrogen peroxide (Figs. 8*C* and 9*B*). Only a part of Reaction 8 may result in the formation of hydroxyl radicals (Reaction 8′). The other may be followed by hydrogen peroxide-consuming reactions (Reactions 9 and 10), the detailed mechanism remaining to be clarified. Rush and Koppenol (52) have suggested the possibility that hydroxyl radicals are formed via Reaction 10. The efficiency of hydroxyl radical formation in the Fenton's reaction is also a problem to be solved (72, 73). The increase of DMPO-OOH formation in the presence of hydrogen peroxide (Table III) can be explained in terms of the decrease in the Fe(II)-EDTA concentration.

4) In the presence of a certain amount of hydrogen peroxide, as shown in Table III, the increase in the rate of superoxide generation brings about a depression in hydroxyl radical production. This depression can be partially removed by increasing the concentration of hydrogen peroxide. Fig. 14*B* shows such competition between Reactions 6 and 8. However, the superoxide-induced destruction of DMPO-OH, recently reported by Samuni *et al.* (74) should also be considered.

Although the results shown in Table III are somewhat complicated, those in the presence of EDTA can be explained by the known kinetic data (Fig. 14*B*). The results with DETAPAC and endogenous chelator, however, cannot be completely explained because of lack of detailed kinetic data. A slight increase of DMPO-OOH formation by hydrogen peroxide in the presence of deferoxamine also remains unexplained. In Table III we consider that $[DMPO\text{-}OH]_{max}$ as measured by ESR is nearly equal to the total amount of DMPO-OH accumulated during the course of the reaction because of the inherent stability of the DMPO-OH adduct while the total amount of DMPO-OOH actually formed is much greater than that measured by ESR as $[DMPO\text{-}OOH]_{max}$ because of the inherent instability of the DMPO-OOH adduct.

It is now clear that spin trapping by DMPO can be used effectively for kinetic analysis of oxygen radicals generated in enzyme reactions even though the reaction of DMPO with superoxide is slow and its product is unstable. The most important criticism to be raised might be that the generation of hydroxyl radicals following superoxide formation is modified by the trapping of superoxide by DMPO as discussed by Britigan *et al.* (65) and Kleinhans and Barefoot (33) in neutrophil systems. New kinetic approaches are necessary to solve this problem, which is now under investigation in this laboratory.

REFERENCES

1. Fridovich, I. (1986) *Arch. Biochem. Biophys.* **247,** 1–11
2. Halliwell, B., and Gutteridge, J. M. C. (1986) *Arch. Biochem. Biophys.* **246,** 501–514
3. McCord, J. M., and Fridovich, I. (1969) *J. Biol. Chem.* **244,** 6049–6055
4. Yamazaki, I., and Piette, L. H. (1963) *Biochim. Biophys. Acta* **77,** 47–64
5. Nakamura, S., and Yamazaki, I. (1969) *Biochim. Biophys. Acta* **189,** 29–37
6. Odajima, T., and Yamazaki, I. (1972) *Biochim. Biophys. Acta* **284,** 355–359
7. Makino, R., Tanaka, T., Iizuka, T., Ishimura, Y., and Kanegasaki, S. (1986) *J. Biol. Chem.* **261,** 11444–11447
8. Kakinuma, K., and Kaneda, M. (1980) *FEBS Lett.* **111,** 90–94
9. Kuthan, H., Ullrich, V., and Estabrook, R. W. (1982) *Biochem. J.* **203,** 551–558
10. Bors, W., Saran, M., Lengfelder, E., Michel, C., Fuchs, C., and Frenzel, C. (1978) *Photochem. Photobiol.* **28,** 629–638
11. Rosen, G. M., Finkelstein, E., and Rauckman, E. J. (1982) *Arch. Biochem. Biophys.* **215,** 367–378
12. Bors, W., Michel, C., and Saran, M. (1979) *Eur. J. Biochem.* **95,** 621–627
13. Baker, M. S., and Gebicki, J. M. (1984) *Arch. Biochem. Biophys.* **234,** 258–264
14. Grootveld, M., and Halliwell, B. (1986) *Biochem. J.* **237,** 499–504
15. Winston, G. W., and Cederbaum, A. I. (1986) *Biochem. Pharmacol.* **35,** 4053–4058
16. Peters, J. H., Gordon, G. R., Kashiwase, D., Lown, J. W., Yen, S. F., and Plambeck, J. A. (1986) *Biochem. Pharmacol.* **35,** 1309–1323
17. Knowles, P. F., Gibson, J. F., Pick, F. M., and Bray, R. C. (1969) *Biochem. J.* **111,** 53–58
18. Ballou, D., Palmer, G., and Massey, V. (1969) *Biochem. Biophys. Res. Commun.* **36,** 898–904
19. Lai, C. S., and Piette, L. H. (1977) *Biochem. Biophys. Res. Commun.* **78,** 51–59
20. Buettner, G. R., and Oberley, L. W. (1978) *Biochem. Biophys. Res. Commun.* **83,** 69–74
21. Finkelstein, E., Rosen, G. M., and Rauckman, E. J. (1980) *Arch. Biochem. Biophys.* **200,** 1–16
22. Buettner, G. R. (1987) *Free Radical Biol. Med.* **3,** 259–303
23. Janzen, E. G., Nutter, D. E., Jr., Davis, E. R., Blackburn, B. J., Poyer, J. L., and McCay, P. B. (1978) *Can. J. Chem.* **56,** 2237–2242
24. Lai, C.-S., and Piette, L. H. (1978) *Arch. Biochem. Biophys.* **190,** 27–38
25. Komiyama, T., Kikuchi, T., and Sugiura, Y. (1982) *Biochem. Pharmacol.* **31,** 3651–3656
26. Floyd, R. A., and Lewis, C. A. (1983) *Biochemistry* **22,** 2645–2649
27. Kalyanaraman, B., Sealy, R. C., and Sinha, B. K. (1984) *Biochim. Biophys. Acta* **799,** 270–275

28. Bowyer, J. R., and Camilleri, P. (1985) *Biochim. Biophys. Acta* **808,** 235-242
29. Moreno, S. N. J., Schreiber, J., and Mason, R. P. (1986) *J. Biol. Chem.* **261,** 7811-7815
30. Morehouse, K. M., and Mason, R. P. (1988) *J. Biol. Chem.* **263,** 1204-1211
31. Finkelstein, E., Rosen, G. M., and Rauckman, E. J. (1980) *J. Am. Chem. Soc.* **102,** 4994-4999
32. Davis, G., and Thornalley, P. T. (1983) *Biochim. Biophys. Acta* **724,** 456-464
33. Kleinhans, F. W., and Barefoot, S. T. (1987) *J. Biol. Chem.* **262,** 12454-12457
34. Finkelstein, E., Rosen, G. M., and Rauckman, E. J. (1982) *Mol. Pharmacol.* **21,** 262-265
35. Fridovich, I. (1970) *J. Biol. Chem.* **245,** 4053-4057
36. Weinstein, J., and Bielski, B. H. (1979) *J. Am. Chem. Soc.* **101,** 58-62
37. Gum, J. R., and Strobel, H. W. (1979) *J. Biol. Chem.* **254,** 4177-4185
38. Morrisett, J. D. (1976) in *Spin Labeling, Theory and Applications* (Berliner, L. J., ed) pp. 272-338, Academic Press, Orlando, FL
39. Sawada, Y., and Yamazaki, I. (1973) *Biochim. Biophys. Acta* **327,** 257-265
40. Winston, G. W., Feierman, D. E., and Cederbaum, A. I. (1984) *Arch. Biochem. Biophys.* **232,** 378-390
41. Winterbourn, C. C., and Sutton, H. C. (1984) *Arch. Biochem. Biophys.* **235,** 116-126
42. Graf, E., Mahoney, J. R., Bryant, R. G., and Eaton, J. W. (1984) *J. Biol. Chem.* **259,** 3620-3624
43. Butler, J., Hoey, B. M., and Swallow, A. J. (1985) *FEBS Lett.* **182,** 95-98
44. Korbashi, P., Kohen, R., Katzhendler, J., and Chevion, M. (1986) *J. Biol. Chem.* **261,** 12472-12476
45. Noguchi, T., and Nakano, M. (1974) *Biochim. Biophys. Acta* **368,** 446-455
46. Harris, D. C., and Aisen, P. (1973) *Biochim. Biophys. Acta* **329,** 156-158
47. Pasternack, R. F., and Halliwell, B. (1979) *J. Am. Chem. Soc.* **101,** 1026-1031
48. McClune, G. J., Fee, J. A., McCluskey, G. A., and Groves, J. T. (1977) *J. Am. Chem. Soc.* **99,** 5220-5222
49. Bull, C., Fee, J. A., O'Neill, P., and Fielden, E. M. (1982) *Arch. Biochem. Biophys.* **215,** 551-555
50. Bull, C., McClune, G. J., and Fee, J. A. (1983) *J. Am. Chem. Soc.* **105,** 5290-5300
51. Walling, C., Partch, R. E., and Weil, T. (1975) *Proc. Natl. Acad. Sci. U. S. A.* **72,** 140-142
52. Rush, J. D., and Koppenol, W. H. (1986) *J. Biol. Chem.* **261,** 6730-6733
53. Rush, J. D., and Koppenol, W. H. (1987) *J. Inorg. Biochem.* **29,** 199-215
54. Diguiseppi, J., and Fridovich, I. (1980) *Arch. Biochem. Biophys.* **203,** 145-150
55. Butler, J., and Halliwell, B. (1982) *Arch. Biochem. Biophys.* **218,** 174-178
56. Piette, L. H., Baxley, L. H., Grover, T. A., and Harwood, P. J. (1984) in *Oxygen Radicals in Chemistry and Biology* (Bors, W., Saran, M., and Tait, D., eds) pp. 137-145, Walter de Gruyter, Berlin
57. Keller, R. J., Coulombe, R. A., Jr., Sharma, R. P., Grover, T. A., and Piette, L. H. (1989) *Free Radical Biol. Med.* **6,** 15-22
58. Bus, J. S., Aust, S. D., and Gibson, J. E. (1974) *Biochem. Biophys. Res. Commun.* **58,** 749-755
59. Misra, H. P., and Gorsky, L. D. (1981) *J. Biol. Chem.* **256,** 9994-9998
60. Bagley, A. C., Krall, J., and Lynch, R. E. (1986) *Proc. Natl. Acad. Sci. U. S. A.* **83,** 3189-3193
61. Elstner, E. F., and Osswald, W. (1980) *Z. Naturforsh. Sect. C Biosci.* **35,** 129-135
62. Hassan, H. M., and Fridovich, I. (1979) *J. Biol. Chem.* **254,** 10846-10852
63. Hassett, D. J., Britigan, B. E., Svendsen, T., Rosen, G. M., and Cohen, M. S. (1987) *J. Biol. Chem.* **262,** 13404-13408
64. Behar, D., Czapski, G., Rabani, J., Dorfman, L. M., and Schwarz, H. A. (1970) *J. Phys. Chem.* **74,** 3209-3213
65. Britigan, B. E., Rosen, G. M., Chai, Y., and Cohen, M. S. (1986) *J. Biol. Chem.* **261,** 4426-4431
66. Halliwell, B. (1985) *Biochem. Pharmacol.* **34,** 229-233
67. Davies, M. J., Donkor, R., Dunster, C. A., Gee, C. A., Jonas, S., and Willson, R. L. (1987) *Biochem. J.* **246,** 725-729
68. Farrington, J. A., Ebert, M., Land, E. J., and Fletcher, K. (1973) *Biochim. Biophys. Acta* **314,** 372-381
69. Ilan, Y. A., and Czapski, G. (1977) *Biochim. Biophys. Acta* **498,** 386-394
70. Levey, G., and Ebbesen, T. W. (1983) *J. Phys. Chem.* **87,** 829-832
71. Sutton, H. C., and Winterbourn, C. C. (1984) *Arch. Biochem. Biophys.* **235,** 106-115
72. Sutton, H. C., Vile, G. F., and Winterbourn, C. C. (1987) *Arch. Biochem. Biophys.* **256,** 462-471
73. Minotti, G., and Aust, S. D. (1987) *J. Biol. Chem.* **262,** 1098-1104
74. Samuni, A., Krishna, C. M., Riesz, P., Finkelstein, E., and Russo, A. (1989) *Free Radical Biol. Med.* **6,** 141-148

SUPPLEMENTARY MATERIAL TO

Kinetic Studies on Spin Trapping of Superoxide and Hydroxyl Radicals Generated in NADPH-Cytochrome P-450 Reductase-Paraquat Systems—Effect of Iron Chelates

Isao Yamazaki*, Lawrence H. Piette, and Thomas A. Grover

MATERIALS AND METHODS

Protease (bromelain)-solubilized NADPH-cytochrome P-450 reductase was prepared from rat liver microsomes with minor modification of the procedures of Gum and Strobel (37). Xanthine oxidase (Grade 1), paraquat, NADPH, xanthine, cytochrome c and DETAPAC were obtained from Sigma Chemical Company. Deferoxamine was obtained from CIBA-Geigy and EDTA from MCB Manufacturing Chemists, Inc. DMPO and 2,2,6,6-tetramethyl-4-hydroxypiperidine (Tempol) were obtained from Aldrich Chemical Company. DMPO was used after re-distilling.

Reactions were carried out at 25° C under aerobic conditions in 0.1 M potassium phosphate buffer (pH 7.4) containing 0.15 M KCl. The volume of reaction solutions was 1.0 ml for both spectrophotometric and ESR assays. Optical absorbance changes were measured with a Beckman DU-7 spectrophotometer equipped for thermostatic control. ESR assays were performed in a flat cell using a Varian E-9 spectrometer. Reactions were started by injecting the mixture (980 µl, preincubated in a water bath at 25° C) to be analyzed into a 20 µl NADPH solution contained in a reservoir connected to the ESR flat cell through a plastic tube. This tube was prefilled with buffer so that after rapid injection, the reaction mixture could be transferred smoothly by negative pressure to the flat cell in the ESR cavity. The ESR measurement was started about 6 s after initiation of the reaction. Room temperature was 21-22° C.

ESR data were collected according to the following three categories: (1) ordinary scan to record entire spectrum; (2) repeat scans of the first portion of the spectrum over the same magnetic field of 10 gauss to follow temporal changes in the spectral pattern. During these scans recording was continuous at a constant rate; and (3) kinetic traces at a fixed magnetic field to follow the time course of a specified absorption line. The rate constant for the reduction of DMPO-OOH by Fe(II)-EDTA was measured using a flow apparatus (Model RX 1000, Applied Photophysics Ltd, England) following the procedure referred to as Category 3 above. DMPO-OOH was produced in one of the two mixing solutions by illumination with water-filtered UV light for 10 seconds just before mixing (56). This solution contained 200 µM riboflavin, 100 µM NADPH, 100 µM EDTA and 100 mM DMPO in the phosphate buffer. Production of DMPO-OOH ceases immediately upon extinguishing the light.

Spin concentrations of DMPO-OOH and DMPO-OH were determined by double integration of their respective ESR signals (Fig. 1) using a 16.2 µM tempol solution as an integration standard. The tempol concentration was determined using the extinction coefficient at 240 nm of 1440 $M^{-1}cm^{-1}$ (38). Spin concentrations in the kinetic traces were determined by comparing peak heights with the standard spectra shown in Fig. 1. The relative concentrations of DMPO-OOH and DMPO-OH in a mixture could be determined by matching the peak heights of resonance lines in the experimental spectrum with those generated by computer simulations as described in the text.

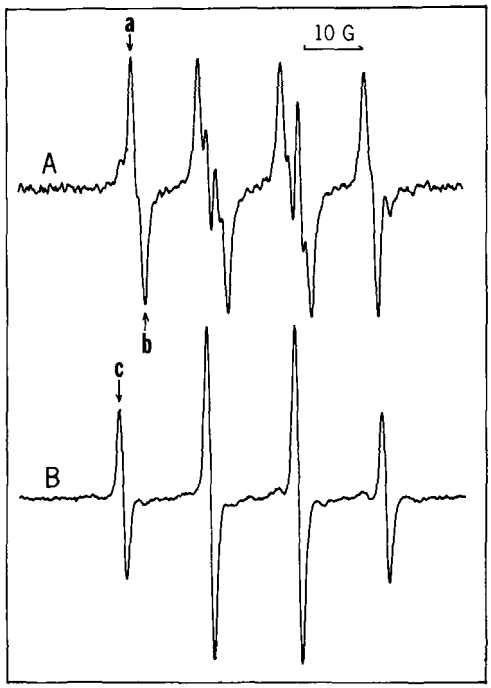

Fig. 1. ESR spectra of DMPO-OOH and DMPO-OH used for determination of the spin concentration. Modulation amplitude = 1 G, scan speed = 25 G/min and time constant = 0.5 s. A, a spectrum obtained 3 min after initiation of the reaction containing 100 μM deferoxamine, 10 μM paraquat, 100 mM DMPO, 100 μM NADPH and 0.2 μM NADPH-cytochrome P-450 reductase. The spectrum was a mixture of 5.8 μM DMPO-OOH and 0.37 μM DMPO-OH, as described later. Signal gain = 8×10^3. B, a spectrum obtained 3 min after initiation of the reaction containing 100 μM EDTA, 5 μM Fe(III) ions, 10 μM paraquat, 1 mM hydrogen peroxide, 100 mM DMPO, 100 μM NADPH, and 0.2 μM NADPH-cytochrome P-450 reductase. Signal gain = 2.5×10^2.

RESULTS

ESR spectra of DMPO-OOH and DMPO-OH used for determination of spin concentrations are shown in Fig. 1. The DMPO-OOH spectrum was obtained from an NADPH-cytochrome P-450 reductase-paraquat system in the presence of deferoxamine. Under our standard experimental conditions in the presence of 0.2 μM enzyme and 10 μM paraquat, the DMPO-OOH concentration reached a maximum level about 3 min after initiation of the reaction. This level of DMPO-OOH lasted for a few minutes and the spectrum in Fig. 1A was recorded during this time. The spin concentration calculated from the spectrum in Fig. 1A was 6.17 μM. As described later, this spectrum contained a 6% contribution from DMPO-OH. The relationship between signal height and spin concentration for DMPO-OOH was determined, so that the rate of DMPO-OOH formation could be measured by following the height at peak a or the depth of valley b shown in Fig. 1A. The ESR spectrum of DMPO-OH was stable and could easily be obtained from an NADPH-cytochrome P-450 reductase-paraquat system in the presence of hydrogen peroxide and Fe(III)-EDTA. The spectrum in Fig. 1B was calculated to have a spin concentration of 6.12 μM.

The formation of DMPO-OH was found to be negligible during the initial stage of reactions in the presence of deferoxamine and formation curves for DMPO-OOH were recorded by monitoring the increase in absorption intensity with the ESR spectrometer fixed at the magnetic field for peak a (Fig. 1A). Figure 2 shows such kinetic traces taken at varying concentrations of paraquat. The ordinate is scaled at μM concentration. The rate of DMPO-OOH formation measured from these traces was plotted against the paraquat concentration in Fig. 3A. In the same figure, the rate of DMPO-OOH formation is compared with the rate of NADPH oxidation measured under identical reaction conditions. The NADPH oxidation increased linearly with the paraquat concentration while the rate of DMPO-OOH formation approached a saturation level (Fig. 3A). If one assumes that paraquat mediates the production of two moles of superoxide per mole of NADPH consumed, it might be concluded from Fig. 3A that under these experimental conditions, DMPO trapped only a portion of the superoxide produced during the reaction. As described in many publications (20, 28, 34), DMPO-OOH is unstable and the level decreases after reaching a maximum. The maximum levels of DMPO-OOH are plotted against the paraquat concentration in Fig. 3B. These data presented two interesting questions: First, is there any relationship between the decay rate and the maximum level of DMPO-OOH attained? and second, can we formulate the effect of the DMPO concentration on the amount of superoxide spin trapped?

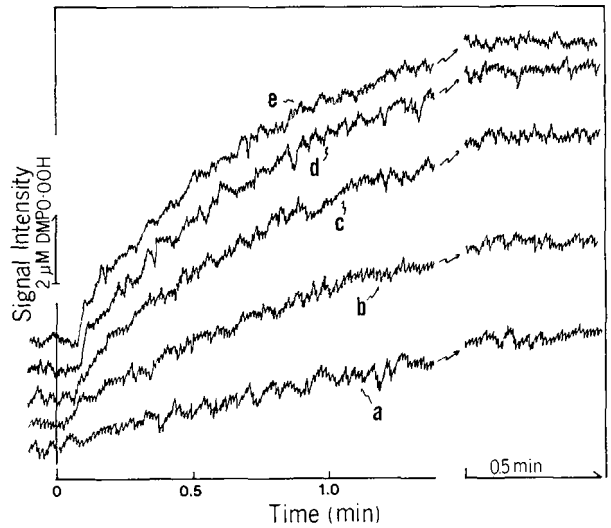

Fig. 2. Formation curves for DMPO-OOH at varying concentrations of paraquat. Magnetic field was fixed on peak a in Fig. 1A. The reaction was started at 0 time in the abscissa. Kinetic traces are interrupted at 1.3 min, followed by traces showing maximum levels of adduct formation (steady state). An apparent lag time of about 6 s seen at high paraquat concentrations was attributed to the time needed to transfer a reaction mixture to the sample cell. Reaction mixtures contained 100 μM deferoxamine, 100 mM DMPO, 100 μM NADPH, 0.2 μM NADPH-cytochrome P-450 reductase, and paraquat at 5 μM for a, 10 μM for b, 20 μM for c, 30 μM for d, or 40 μM for e.

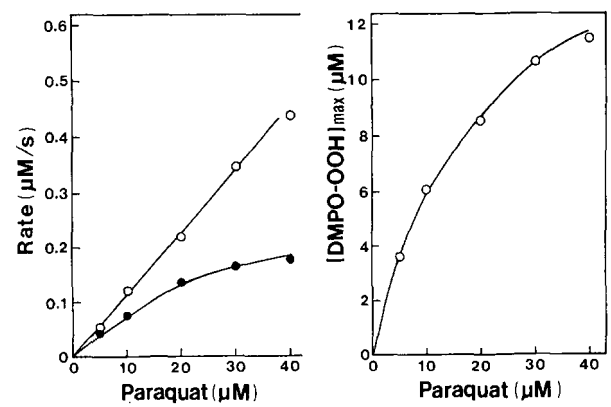

Fig. 3. Relation between the oxidation of NADPH and the formation of DMPO-OOH. Conditions were the same as described in Fig. 2. The rate of NADPH oxidation was measured spectrophotometrically at 340 nm. A, the rates of NADPH oxidation (o) and DMPO-OOH formation (●) are plotted against paraquat concentration. B, the maximum levels of DMPO-OOH attained at specified paraquat concentrations.

The half decay time of DMPO-OOH has been reported to be pH dependent (20), being 35 s (pH 8), 60 s (pH 7) and 2 min (pH 7.4) in photochemical (20), photobiological (28) and chemical (34) systems at room temperature, respectively. Figure 4 shows kinetic curves for appearance and disappearance of DMPO-OOH in the NADPH-cytochrome P-450 reductase system containing a relatively high amount of paraquat. Here, the DMPO-OOH concentration was followed at valley b in Fig. 1A for the reasons described later. Time courses of NADPH oxidation are shown in the same figure. After the disappearance of NADPH, DMPO-OOH decayed according to first order kinetics with a half time of 66 s. This value is consistent with that obtained from a photobiological system (28). We examined the possibility that the maximum level of DMPO-OOH is determined by the following simple equation:

$$v_s = k_1 [\text{DMPO-OOH}]_{max} \quad (1)$$

where k_1 is the first order rate constant and v_s denotes the rate of DMPO-OOH formation at the time when the DMPO-OOH level reaches a maximum (steady state). Using Equation 1 we can calculate k_1 from the data in Fig. 3 (Table I). The half decay time of 66 s was found to be consistent with a rate constant of 0.011 s^{-1} obtained at paraquat concentrations of 5 and 10 μM. As the paraquat concentration increased, the decay rate increased slightly probably because of additional decay of DMPO-OOH through direct reduction by the superoxide or paraquat radical.

TABLE I
Rate constant for DMPO-OOH decay calculated with Equation 1. Conditions were as described in Fig. 2.

Paraquat (μM)	Time[a] (min)	Rate (μM/s)[b] NADPH oxidation	DMPO-OOH formation	$[\text{DMPO-OOH}]_{max}$ (μM)	k_1 (s^{-1})
5	3	c)	0.040	3.60	0.011
10	3	0.110	0.071	6.20	0.011
20	2.5	0.188	0.112	8.58	0.013
30	2	0.262	0.145	10.73	0.014
40	2	0.322	0.160	11.50	0.014

[a] Time when [DMPO-OOH] reaches maximum.
[b] The rate of NADPH oxidation was measured at time a and then that of DMPO-OOH formation was obtained using the data shown in Fig. 3A.
[c] The initial rate of NADPH oxidation remained constant during 3 min.

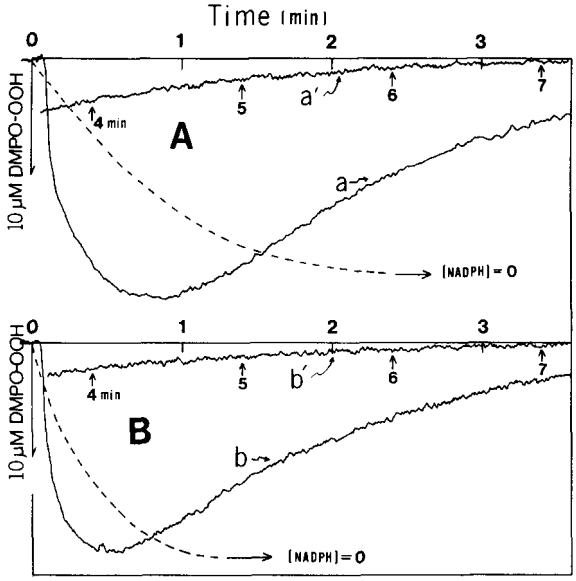

Fig. 4. Formation and decay of DMPO-OOH. Magnetic field was set at valley p in Fig. 1A (see RESULTS). NADPH oxidation versus time is shown with broken lines. Reaction mixtures contained 100 μM deferoxamine, 100 mM DMPO, 400 μM paraquat, 100 μM NADPH and 0.2 μM (A) or 0.4 μM (B) NADPH-cytochrome P-450 reductase. The end of traces a and b continues to a' and b', respectively.

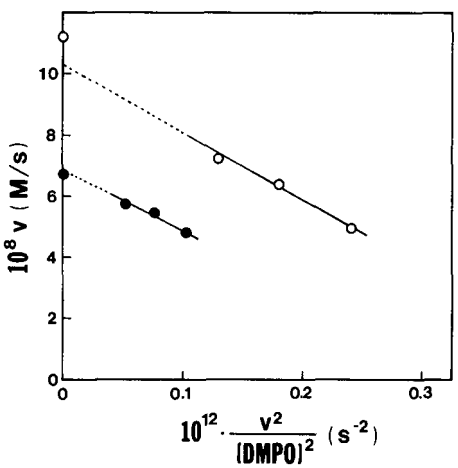

Fig. 5. Effects of DMPO concentration on the rate of DMPO-OOH formation. Plotted from data in Table II. NADPH-cytochrome P-450 reductase (o) and xanthine oxidase (e). The values on the ordinate were obtained from the rate of NADPH oxidation (o) and the rate of cytochrome c reduction (e).

TABLE II

Effect of DMPO concentration on the rate of DMPO-OOH formation (v) in the NADPH-cytochrome P-450 reductase and xanthine oxidase systems.

DMPO (mM)	NADPH-cytochrome P-450 reductase[a], v (μM/s)	Xanthine oxidase[b] v (μM/s)
100	0.049	0.035
150	0.064	0.048
200	0.072	0.055

[a] 100 μM deferoxamine, 5 μM paraquat, 100 μM NADPH, and 0.2 μM NADPH-cytochrome P-450 reductase. The rate of NADPH oxidation was 0.056 μM/s.
[b] 100 μM deferoxamine, 200 μM xanthine, 0.03 unit xanthine oxidase/ml. The rate of cytochrome c reduction in the presence of 50-100 μM cytochrome c was 0.068 μM/s.

It seemed reasonable that DMPO-OOH accumulation increased with the DMPO concentration in a superoxide generating system. DMPO had no inhibitory effect on the NADPH-cytochrome P-450 reductase-paraquat reaction. The dependence of the rate of DMPO-OOH formation on DMPO concentration was analyzed using the following equation, which has been applied to similar reaction systems (31, 39).

$$v = k_2 [O_2^{\cdot-}] [DMPO] + k_d [O_2^{\cdot-}]^2 \quad (2)$$

Here it was assumed that superoxide ions disappear only through reactions with DMPO and dismutation. The rate of superoxide formation (V) is then equal to the sum of the two rates of reaction of superoxide at steady state. Putting v for $k_2 [O_2^{\cdot-}][DMPO]$, one can obtain the following equation,

$$v = V - k_d/k_2^2 \cdot v^2/[DMPO]^2 \quad (3)$$

In Fig. 5, v is plotted against $v^2/[DMPO]^2$. In order to confirm the reliability of this kinetic analysis, a similar experiment was carried out with a xanthine oxidase system and the result is also shown in Fig. 5. Values of V could be measured independently for both reactions (Table II) and are plotted on the ordinate axis in Fig. 5. These quantitative analyses clearly indicate that v obtained by extrapolation to infinite [DMPO] was equal to the rate of superoxide production measured from the reduction of cytochrome c in the xanthine oxidase system and to about twice the rate of NADPH oxidation in the NADPH-cytochrome P-450 reductase-paraquat system.

The above kinetic studies on the formation of DMPO-OOH were carried out in the presence of deferoxamine in order to inhibit iron-involved Fenton reactions that ultimately convert superoxide into hydroxyl radical. This inhibition by deferoxamine has been reported in xanthine oxidase systems (40-42), NADPH-cytochrome P-450 reductase sytems (40, 43) and E. coli systems (44). It was evident from Fig. 6A, however, that a small amount of DMPO-OH appears 3 min after initiation of the reaction and lasted for a long time. A DMPO-OH spectrum was clearly observed following the disappearance of DMPO-OOH (Fig. 6B). The DMPO-OH concentration was calculated to be 0.80 μM, which was 6% of the maximal level of DMPO-OOH accumulated. We concluded that the DMPO-OH spectrum was the result of the reaction of DMPO with hydroxyl radicals and not the result of direct conversion from DMPO-OOH to DMPO-OH, since in the presence of 0.4 M ethanol the DMPO-adduct of the ethanol radical appeared instead of DMPO-OH (Fig. 6C). A similar result has been reported by Finkelstein et al. (34) in a system containing a superoxide salt.

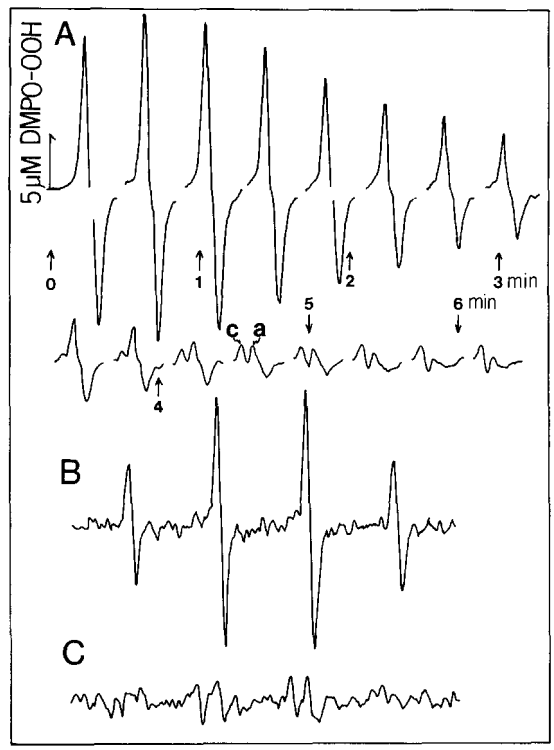

Fig. 6. Effect of ethanol on the residual DMPO-OH appearing during the spin trapping of superoxide. The reaction mixture was the same as described in Fig. 4A. A, the first portion of spectrum was recorded according to Category 2 (see MATERIALS AND METHODS) at gain = 4×10^4. B, the complete spectrum was recorded at gain = 1.25×10^5, 7 min after initiation of the reaction. C, the same as B, except that 0.4 M ethanol was present at the start of the reaction.

We thought it worthwhile to extend these quantitative analyses to the iron-catalyzed Haber-Weiss reaction. The role of iron in the NADPH-cytochrome P-450 reductase system appeared to be complex since there was the possibility of Fe(III) ions serving as direct electron acceptors for the ensyme (40, 45). Figure 7 shows distinct differences in the reactions of NADPH-cytochrome P-450 reductase with Fe(III) complexes of deferoxamine, DETAPAC and EDTA. Fe(III)-deferoxamine was inactive with the enzyme. Fe(III)-DETAPAC and Fe(III)-EDTA were both reduced by the enzyme although the role of chelators was different. Fe(III)-DETAPAC was reduced faster than Fe(III)-EDTA. The stoichiometric reduction of Fe(III)-DETAPAC indicates that the autooxidation of Fe(II)-DETAPAC was very slow as reported previously (40, 42). NADPH was oxidized beyond the stoichiometric amount of added Fe(III)-EDTA. This result is reasonable because Fe(II)-EDTA is autooxidizable (46).

These Fe(III)-complexes acted quite differently also in the paraquat-mediated superoxide producing system. Figure 8 shows the differences observed in the presence of 5 μM Fe(III) ions. With deferoxamine very little DMPO-OH is observed over the course of the reaction (Fig. 8A). DETAPAC accelerated the formation of DMPO-OH, but the reaction pattern was similar to that without DETAPAC. That is, both in the presence and absence of DETAPAC, the DMPO-OOH formation was slightly decreased as compared with that in the presence of deferoxamine and the DMPO-OH signal increased significantly as the reaction proceeded (Fig. 8B). In contrast to the above two chelators, EDTA strongly inhibited the accumulation of DMPO-OH as well as DMPO-OOH (Fig. 8C). The inhibition might be explained in terms of superoxide dismutase-like (47-50) and pseudo catalase-like (51-53) activities of Fe(III)-EDTA but its superoxide dismutase activity is still a matter of controversy (54-55) as discussed later. Since the reductive decomposition of DMPO-OOH by Fe(II)-EDTA had been suggested by Pietta et al. (56), the rate constant for the reaction of DMPO-OOH with Fe(II)-EDTA was measured by stopped flow ESR methods (see Materials and Methods). The reaction was started by mixing 4 μM DMPO-OOH solution with 25 to 100 μM ferrous ammonium sulfate solution freshly diluted from its anaerobic stock solution. The rate of DMPO-OOH decay was proportional to the ferrous concentration, giving a rate constant of 6×10^4 $M^{-1}s^{-1}$ for the reduction of DMPO-OOH by Fe(II)-EDTA if the Fe(II)-EDTA complex is assumed to be formed within one second.

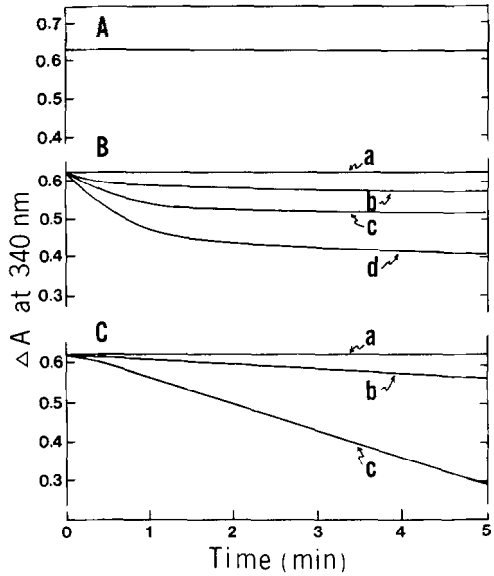

Fig. 7. Roles of Fe(III)-chelator complexes in the NADPH-cytochrome P-450 reductase system. Each reaction mixture contained 100 μM chelator, 100 μM NADPH and 0.2 μM enzyme. A, deferoxamine and 60 μM Fe(III) ions. B, DETAPAC and 0 μM (a), 5 μM (b), 25 μM (c), or 60 μM (d) Fe(III) ions. C, EDTA and 0 μM (a), 5 μM (b) or 60 μM (c) Fe(III) ions.

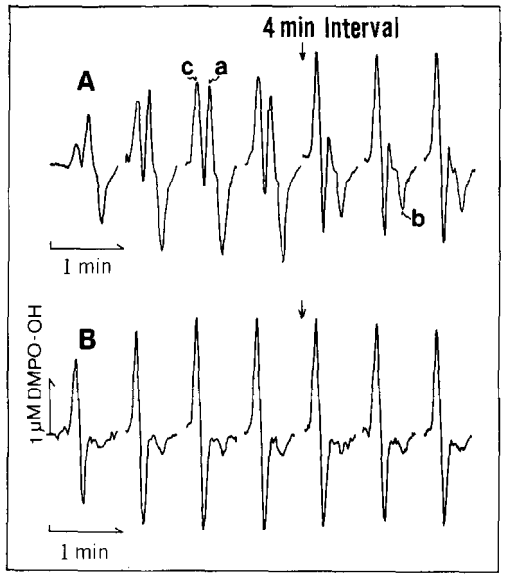

Fig. 9. Formation of DMPO-OOH and DMPO-OH in the presence of added hydrogen peroxide. The conditions were as described in Fig. 8 except for the addition of 100 μM hydrogen peroxide. A, for DETAPAC and B, for EDTA.

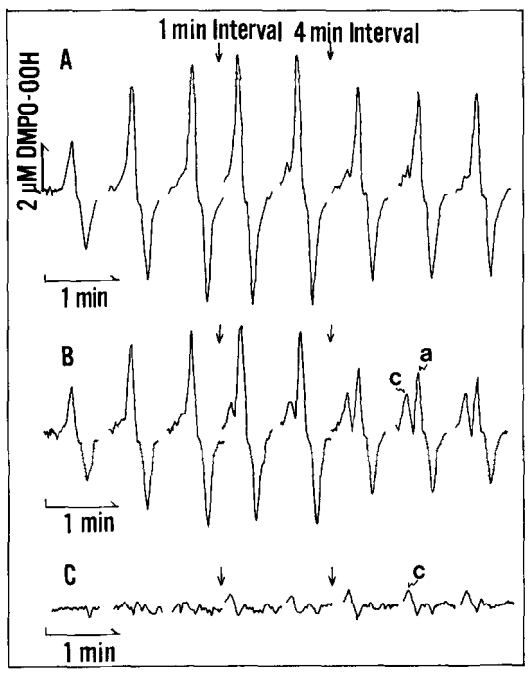

Fig. 8. Effect of chelators on the formation of DMPO-OOH. Each reaction mixture contained 100 μM chelator, 5 μM Fe(III) ions, 100 mM DMPO, 10 μM paraquat, 100 μM NADPH and 0.2 μM NADPH-cytochrome P-450 reductase. The spectra were recorded according to Category 2 (see MATERIALS AND METHODS) at gain = 8×10^2. Some intermediate spectra were skipped at arrows. A, for deferoxamine, B, for DETAPAC, and C, for EDTA.

Similar experiments to those in Fig. 8 were performed in the presence of 5 μM Fe(III) ions and 100 μM hydrogen peroxide. When deferoxamine was present, the addition of hydrogen peroxide did not alter the reaction pattern shown in Fig. 8A. However, with DETAPAC and EDTA the accumulation of DMPO-OH was greatly accelerated (Fig. 9). In particular, with EDTA, only DMPO-OH was observed from the beginning of the reaction (Fig. 9B). Even in this case the amount of DMPO-OH detected was less than one-third that of DMPO-OOH accumulated in the presence of deferoxamine (Table III).

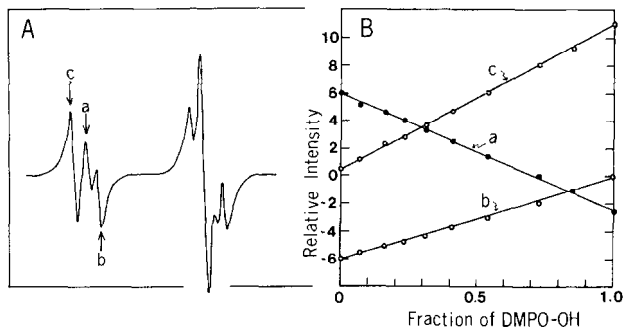

Fig. 10. Plots derived from computer-simulated ESR spectra of DMPO-OOH and DMPO-OH mixed in different ratios. A, upfield half of the ESR spectrum that results from a mixture of 59% DMPO-OOH and 41% DMPO-OH. B, plots of the relative intensities of resonance positions a, b, and c as a function of molar fraction of DMPO-OH (x). The relative intensity at each resonance position (a, b, or c) can be calculated as 6 - 8.4x for a, -6 + 6x for b, and 0.5 + 10.4x for c.

In order to measure concentrations of DMPO-OOH and DMPO-OH in mixtures of the two, we used a computer simulation of the two species with varying mixture percentage using just the first portion of the spectrum (Fig. 10). As the fraction of DMPO-OH increased in a mixture, we observed a linear increase in the height of peak c and linear decreases in the height of peak a and the depth of valley b. Using this result we could easily measure the molar fraction of DMPO-OH to be 0.06 in the reaction mixture that yielded the ESR spectrum shown in Fig. 1A. There remains, however, a problem as to why the height of peak a is a little higher than the depth of valley b in Fig. 1A. Computer analysis clearly showed that this should be the reverse. At any rate, peak a could be used for the measurement of the initial rate of DMPO-OOH formation in the presence of deferoxamine. But, for kinetic analysis of DMPO-OH in mixtures with a high ratio of [DMPO-OH] to [DMPO-OOH], as shown in the tail of the traces in Fig. 4, we had to set the magnetic field at valley b instead of peak a.

In the reaction system used in these studies, Fe(III)-EDTA has diverse functions: inhibiting the accumulation of oxygen radicals (Fig. 8C), activating the Haber-Weiss reaction (Fig. 9B), and mediating the O_2 consuming NADPH oxidation (Fig 7C). The effect of increasing Fe(III)-EDTA on the first two functions was studied in reaction mixtures containing 50 μM paraquat. In this case NADPH oxidation was thought to occur mostly through mediation by paraquat even in the presence of 5 μM Fe(III)-EDTA (compare Figs. 3A and 7C). The rate of NADPH oxidation was about 5 times faster in these reactions than in those shown in Figs. 8C and 9B. Under these conditions we needed higher concentrations of Fe(III)-EDTA to suppress the formation of DMPO-OOH in the reactions without added hydrogen peroxide. The concentration of added Fe(III) ions that reduced the DMPO-OOH accumulation to one half in the presence of 100 μM EDTA was 2.7 μM (Fig. 11A). Repeat scans in the reaction with 4 μM Fe(III) ions (Fig. 11B) showed that the first line was irregularly weak, indicating that there was a slight lag in the accumulation of DMPO-OOH. Only DMPO-OOH was observed in the early stage of the reaction and DMPO-OH appeared about 1 min after initiation of the reaction. Figure 11C shows a spectrum taken 4 min after the reaction began, which was interpreted to be a mixture of 3.5 μM DMPO-OOH and 0.4 μM DMPO-OH.

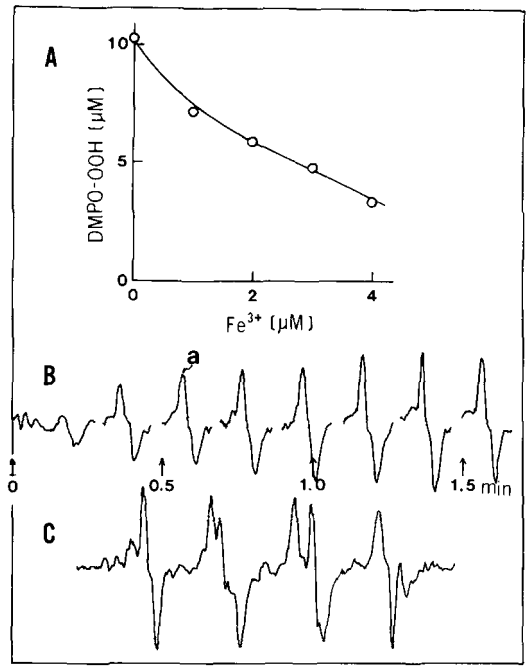

Fig. 11. Effect of the Fe(III)-EDTA concentration on the DMPO-OOH accumulation. Reaction mixtures contained 100 μM EDTA, 100 mM DMPO, 50 μM paraquat, 100 μM NADPH, 0.2 μM NADPH-cytochrome P-450 reductase, and varying amounts of Fe(III) ions. A, maximum levels of DMPO-OOH accumulation were plotted against Fe(III) ion concentration. B, spectra were recorded for the case of 4 μM Fe(III) ions according to Category 2 (see MATERIALS AND METHODS). C, complete spectrum recorded 4 min after initiation of the reaction in B.

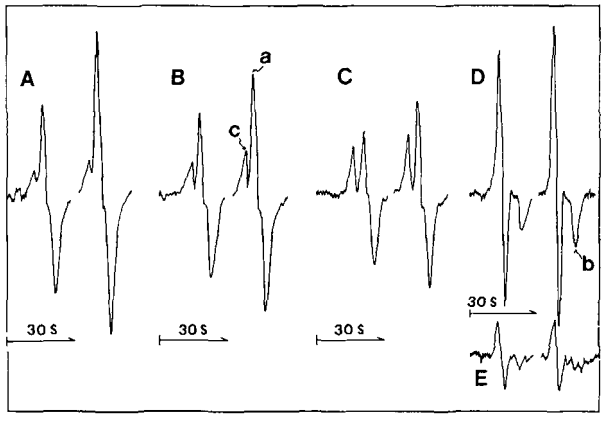

Fig. 12. Effect of Fe(III) ion concentration on the radical species trapped by DMPO in the presence of EDTA and added hydrogen peroxide. The conditions were as described in Fig. 11 except for the presence of added hydrogen peroxide. The hydrogen peroxide concentration was 1 mM for A, B, C, and D, and 200 μM for E. The concentration of added Fe(III) ions was 0 for A, 1 μM for B, 2 μM for C, and 5 μM for D and E.

When 1 mM hydrogen peroxide was present, the effect of Fe(III) ion concentration became dramatic as shown in Fig. 12. Upon the addition of 5 μM Fe(III) ions, peak a was no longer observed in the early stage of the reaction, but the existence of valley b clearly indicated the formation of DMPO-OOH (Fig. 12D). Under these conditions, the formation of DMPO-OOH and DMPO-OH was too fast to measure the exact rates by our present method. It can be roughly said that both DMPO-OOH and DMPO-OH reached their maxima in a minute. Then, DMPO-OOH disappeared gradually while DMPO-OH remained at a maximum level following the complete disappearance of DMPO-OOH. In Fig. 13, their maximum levels were plotted against the concentration of added Fe(III) ion. In this case, the concentration of added Fe(III) ion that reduced the DMPO-OOH accumulation to one half was 3.5 μM. The linear dependence of the maximum level of DMPO-OH on the Fe(III) ion concentration seems to be important because this amount may virtually equal the total amount of DMPO-OH formed during the reaction. It might be suggested by extrapolating the linear line that the phosphate buffer contained 0.9 μM Fe(III) ions as a contaminant. But, we cannot exclude the possibility that some of the DMPO-OH detected at [Fe(III) ion] = 0 originated from decomposition of DMPO-OOH, as described in Fig. 6. In the presence of 1 mM hydrogen peroxide, NADPH-cytochrome P-450 reductase catalyzed the Fe(III)-EDTA-mediated oxidation of NADPH at a fairly high rate. In this system the NADPH oxidation was strongly inhibited by DMPO. Since DMPO had no inhibitory effect on paraquat-mediated NADPH oxidation catalyzed by NADPH-cytochrome P-450 reductase, this inhibition by DMPO suggested involvement of a chain reaction initiated by hydroxyl radicals in the Fe(III)-EDTA-mediated oxidation of NADPH. A similar type of chain reaction inhibited by DMPO has been reported by us (57) in the vanadyl catalyzed oxidation of NADH.

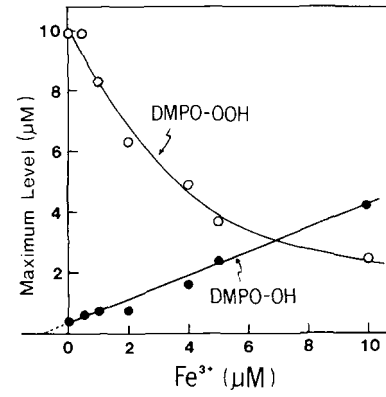

Fig. 13. Effect of Fe(III) ion concentration on the maximum levels of accumulated DMPO-OOH and DMPO-OH. Reaction mixtures contained 100 μM EDTA, varying amounts of Fe(III) ions, 100 mM DMPO, 50 μM paraquat, 1 mM hydrogen peroxide, 100 μM NADPH, and 0.2 μM NADPH-cytochrome P-450 reductase. Data were obtained from similar experiments shown in Fig. 12.

TABLE III

Effect of chelators on the maximum accumulation of DMPO-OOH and DMPO-OH. Conditions were: 100 μM NADPH, 0.2 μM NADPH-cytochrome P-450 reductase, 100 mM DMPO, 5 μM Fe(III) ions added, and 100 μM chelator.

Chelator added	Paraquat (μM)	H_2O_2 added (μM)	$[DMPO\text{-}OOH]_{max}$ (μM)	$[DMPO\text{-}OH]_{max}$ (μM)
No	10	0	2.7	0.6
	10	100	3.8	0.8
Deferoxamine	10	0	5.8	0.4
	10	100	7.0	0.4
DETAPAC	10	0	4.8	0.7
	10	100	4.0	2.0
EDTA	10	0	0	0.2
	10	100	0.7	1.9
	10	1000	0.8	6.1
	50	200	0.4	0.8
	50	1000	2.7	3.4